Scalar electromagnetic propagation modelling using parabolic equations and the split-step Pade approximation

1995 J. Phys. A: Math. Gen. 28 2065

(http://iopscience.iop.org/0305-4470/28/7/025)

J. Phys. A: Math. Gen. 28 (1995) 2065–2080. Printed in the UK

Scalar electromagnetic propagation modelling using parabolic equations and the split-step Padé approximation

Ronald I Brent† and Joseph F A Ormsby‡

† Department of Mathematical Sciences, University of Massachusetts Lowell, Lowell, MA 01854, USA

‡ Joint Command and Control Warfare Center, Kelly AFB, San Antonio TX 78243, USA

Received 18 October 1994

Abstract. This paper presents a solution of 2D electromagnetic wave propagation problems in complicated terrestrial domains. Scalar 2D parabolic approximations are derived from Maxwell's equations for both vertical and horizontal polarization. The parabolic equations are then solved using a new technique involving Padé rational function approximations of the macroscopic operator. This method allows for larger-than-normal range stepping, speeding up computational time significantly. The Padé approximation and the numerical implementation are fully discussed. The discontinuity at the earth's surface is handled directly by using classical continuity conditions and deriving exact interface conditions for linking the fields in the atmosphere to those in the terrain. The interface conditions are then implemented using the concept of virtual points. Preliminary benchmark tests show the interface treatment to work well. Finally, several example runs are presented illustrating results.

1. Introduction

The solution of electromagnetic (EM) propagation problems in the terrestrial domain is a complicated matter. Three-dimensional (3D) variations in refraction and terrain make the full vector problem extremely difficult to solve in reasonable time. If one chooses to simplify the problem by assuming symmetry in one or more of the coordinate directions, the vector problem can be uncoupled into two scalar problems [1]. However, the solution of the two-dimensional (2D) scalar problem is still very difficult for realistic environments. The parabolic approximation method is used to reduce the solution of the full two-way wave equation to a solution of a one-way equation [2]. Benefits of one-way propagation are the simple numerical implementation of range dependencies in the medium, and the avoidance of prohibitive numerical aspects of solving elliptic equations associated with implementing two range-dependent boundary conditions. The model discussed in this paper is a so called 2.5D model using azimuthally varied vertical planar fields. Work is also proceeding on a 3D model for higher frequencies using a hybrid combination of an underlying robust 3D ray trace and a 3D Gaussian beam model.

Two of the most popular methods of solving the parabolic equations are the implicit finite difference (IFD) method [3] and the split-step Fourier transform method [4, 5]. These techniques are microscopic methods in the sense that they are implementing approximations to the differential equation, defined microscopically. Limitations of these methods are that the grid mesh over which the solution is computed must be small to yield accuracy. This often means grid sizes on the scale of at most three wavelengths. At high frequencies and large propagation domains this could amount to grid sizes of hundreds of thousands by

0305-4470/95/072065+16$19.50

millions of points needed for an accurate solution. Methods using fourth-order difference schemes have also been implemented to speed up computational time [6]. A better method to solve the equations is by symbolically integrating the equation with respect to range thereby obtaining the macroscopic propagator [7]. In theory if one does an 'infinitely' good job at approximating the macroscopic propagator it is possible to take 'infinitely' large range steps. Limitations in adequate range-dependent representation of the macroscopic operator, however, will limit actual range step sizes. In practice one still can achieve great savings in computational time over IFD and even possibly the split-step Fourier transform.

The macroscopic operator is approximated using a Padé rational function series. The more terms used in the approximation, theoretically the larger the range-step one can take. Another advantage of this method is that once the Padé approximation for the propagator has been obtained computations may be applied in parallel. That is, each of the n Padé approximations may be applied to the field at the same time as opposed to having to apply a series of products of operators sequentially. For cases when the desired result is the loss values only near the receiver, and not at many points in-between the source and receiver, the Padé technique applied to the macroscopic operator is ideal. It cuts down the number of intermediate range locations at which the field must be computed. It is reiterated, however, that the terrain elevation and cover will ultimately determine the range step size.

This report summarizes the theory involved in deriving parabolic approximations to scalar EM propagation and the associated boundary modelling, including energy conservation at vertical interfaces. Also presented is the theory behind the Padé rational function approximation to the propagator, and the complete numerical implementation used in the code SSP. We first begin with the derivation of scalar wave equations for EM propagation.

2. Derivation of scalar wave equations

We begin with Maxwell's equations [1] in spherical coordinates (r, θ, ϕ), for terrestrial systems where r is the radial distance from the origin, θ (measured positive down,) is the angle between the z-axis and the radial direction and ϕ is the azimuthal angle. Maintaining $\boldsymbol{E}$ planar in the (r, θ) plane leads to $\partial_\phi \boldsymbol{H} = \partial_\phi \varepsilon = 0$ for vertical polarization and $\boldsymbol{H}$ planar in the (r, θ) plane leads to $\partial_\phi \boldsymbol{E} = \partial_\phi \varepsilon = 0$ for horizontal polarization. The assumption of symmetry in the ϕ direction is a necessary requirement to reduce the original vector problem to uncoupled scalar problems.

These assumptions used in Maxwell's equations readily lead to the two equations

$$\frac{n^2}{r}\frac{\partial}{\partial r}\left(\frac{1}{n^2}\frac{\partial}{\partial r}(rH_\phi)\right)+\frac{n^2}{r^2\sin\theta}\frac{\partial}{\partial\theta}\left(\frac{\sin\theta}{n^2}\frac{\partial H_\phi}{\partial\theta}\right)+\left(k_0^2n^2-\frac{1}{r^2\sin^2\theta}-\frac{\cot\theta}{r^2n^2}\frac{\partial n^2}{\partial\theta}\right)H_\phi=0 \tag{1a}$$

and

$$\frac{1}{r}\frac{\partial^2}{\partial r^2}(rE_\phi)+\frac{1}{r^2\sin\theta}\frac{\partial}{\partial\theta}\left(\sin\theta\frac{\partial E_\phi}{\partial\theta}\right)+\left(k_0^2n^2-\frac{1}{r^2\sin^2\theta}\right)E_\phi=0 \tag{1b}$$

where n is the index of refraction defined as

$$n^2=\frac{\varepsilon}{\varepsilon_0}=\left(\frac{c_0}{c}\right)^2+\frac{\mathrm{i}\sigma}{\omega\varepsilon_0}. \tag{1c}$$

Equation (1*a*) determines the only non-zero component of H in the vertical polarization case. Components of E are determined in terms of H_ϕ using Maxwell's equations. Similarly, equation (1*b*) determines the non-zero component of E in the horizontal polarization case. Components of H can then be determined in terms of E_ϕ using Maxwell's equations. This last equation (1*c*) reflects the inclusion of conductivity via current density terms retained in Maxwell's equations.

One may transform equations (1*a*) and (1*b*) into Helmholtz forms by using the substitutions

$$H_\phi = \frac{nu_V}{\sqrt{r\sin\theta}} \quad \text{and} \quad E_\phi = \frac{u_H}{\sqrt{r\sin\theta}}. \tag{2a, b}$$

In doing so, equation (1) yields

$$\frac{1}{r}\frac{\partial}{\partial r}\left(r\frac{\partial u_i}{\partial r}\right) + \frac{1}{r^2}\frac{\partial^2 u_i}{\partial\theta^2} + \left(k_0^2 n^2 - \frac{3}{4r^2\sin^2\theta} + \delta n_i\right)u_i = 0 \tag{3a}$$

where

$$\delta n_i = \begin{cases} -\dfrac{\cot\theta}{r^2 n}\dfrac{\partial n}{\partial\theta} - \dfrac{n}{r^2}\dfrac{\partial^2 n^{-1}}{\partial\theta^2} - n\dfrac{\partial^2 n^{-1}}{\partial r^2} & \text{for } i \equiv V \\ 0 & \text{for } i \equiv H. \end{cases} \tag{3b}$$

We use the subscript notation $i \equiv V (i \equiv H)$ to denote the vertical (horizontal) polarization.

Since the computation of rectangular domains is more desirable than spherical domains, we now present an 'earth-flattening' approximation to our problem. We will use the smooth earth transformation

$$x = r_e\theta \quad \text{and} \quad z = r_e \ln\left(\frac{r}{r_e}\right) \tag{4a, b}$$

where r_e is the radius of the earth at mean sea level (approximately 6370 km). This transformation places the smooth earth's surface at $z = 0$. Terrain will be imposed later during the numerical implementation of the solution algorithm. The inverse transform is given by

$$r = r_e \exp\left(\frac{z}{r_e}\right) \quad \text{and} \quad \theta = \frac{x}{r_e}. \tag{5a, b}$$

In using the transformation defined in equation (4) differential operators translate as

$$\frac{\partial}{\partial\theta} \to r_e\frac{\partial}{\partial x} \quad \text{and} \quad \frac{\partial}{\partial r} \to \exp\left(-\frac{z}{r_e}\right)\frac{\partial}{\partial z}. \tag{6a, b}$$

Equation (3) thereby becomes

$$\frac{\partial^2 u_i}{\partial x^2} + \frac{\partial^2 u_i}{\partial z^2} + \left(k_0^2 m^2 - \frac{3\,\mathrm{cosec}^2(x/r_e)}{4r_e^2} - \delta m_i\right)u_i = 0 \tag{7a}$$

where m is a modified index of refraction defined as

$$m = n\exp\left(\frac{z}{r_e}\right) \tag{7b}$$

and

$$\delta m_i = \begin{cases} -\dfrac{\cot(x/r_e)}{r_e m}\dfrac{\partial m}{\partial x} - m\dfrac{\partial^2 m^{-1}}{\partial x^2} - \dfrac{m}{r_e}\dfrac{\partial m^{-1}}{\partial z} - m\dfrac{\partial^2 m^{-1}}{\partial z^2} & i \equiv \mathrm{V} \\ 0 & i \equiv \mathrm{H}. \end{cases} \tag{7c}$$

The solution of equation (7*a*) using parabolic approximation techniques relies on segmenting the medium into a series of range independent sectors. It can be shown that in each of these sectors equation (7*a*) becomes

$$\frac{\partial^2 u_i}{\partial x^2} + \frac{\partial^2 u_i}{\partial z^2} + K_i^2 u_i = 0 \tag{8a}$$

where

$$K_i^2 = \begin{cases} k_0^2 m^2 - \dfrac{m}{r_e}\dfrac{\partial m^{-1}}{\partial z} - m\dfrac{\partial^2 m^{-1}}{\partial z^2} & i \equiv \mathrm{V} \\ k_0^2 m^2 & i \equiv \mathrm{H} \end{cases} \tag{8b}$$

and the assumption of $z/r_e \ll 1$ is used. We have also neglected the range-dependent $\mathrm{cosec}^2(*)$ term by assuming we are in the far field $k_0 r \gg 1$ and removed from any poles of the cosecant function ($x < \pi r_e$) [8]. Equation (8) is the desired starting equation for numerical implementation. We remark that modelling of media with finite conductivity is achieved by replacing m^2 with the expression

$$m^2 = \left(\frac{c_0}{c_m}\right)^2 + \frac{i\sigma_m}{\omega\varepsilon_0} \tag{9a}$$

where c_m and σ_m are modified light speed and conductivity defined as

$$c_m = c\exp(-z/r_e) \qquad \text{and} \qquad \sigma_m = \sigma\exp(2z/r_e). \tag{9b, c}$$

The next section will discuss the boundary modelling including the effects and corrections for discontinuities in range.

3. Electromagnetic boundary modelling

Since we are solving a parabolic equation with two z derivatives and one x derivative, we need two conditions in z and one condition in x at every range step. Computationally we will bound the domain by two horizontal planes at the top of the atmosphere and the bottom of the terrain. Homogeneous Dirichlet conditions will be used at these boundaries and techniques will be applied to reduce fictitious reflections. The fact that the terrain introduces a discontinuity in the problem, and its elevation is range dependent, complicates the problem slightly. Parabolic approximations assume that range-dependent environments are partitioned into range-independent sectors. The result is that terrain slopes are approximated by a series of step-like structures. This creates a vertical interface at each range step where the terrain elevation is altered significantly enough. Typically, the condition at vertical interfaces is continuity of field, however this is not the best condition one might impose.

We will eventually impose a conservation of energy condition at discontinuities in range to correct for some range-dependent errors.

We first discuss the modelling of the horizontal interface between the atmosphere and the earth's surface. Assuming finite conductivity and no surface charge density the conditions on $\boldsymbol{B}$, $\boldsymbol{H}$, $\boldsymbol{D}$ and $\boldsymbol{E}$, at an interface between two different media (ε_a, μ_a, σ_a) and (ε_b, μ_b, σ_b) are given in [1]. In the case of a smooth interface, the normal vector $e_n = e_r$. Assuming also that magnetic permeability in the terrain is that of the atmosphere (both equal to the free space value,) these conditions imply the following six relations hold:

$$E_{\phi a} = E_{\phi b} \qquad E_{\theta a} = E_{\theta b} \qquad E_{ra} = \frac{\varepsilon_b}{\varepsilon_a} E_{rb} \tag{10a, b, c}$$

$$H_{\phi a} = H_{\phi b} \qquad H_{\theta a} = H_{\theta b} \qquad \text{and} \qquad H_{ra} = H_{rb}. \tag{10d, e, f}$$

For efficient numerical computation, the approach here treats the variable terrain as a series of discrete vertical jumps, i.e. a staircase approximation, using smooth earth formulae for the horizontal boundary conditions in each sector. However, the general boundary conditions for the variable terrain have been determined for vertical and horizontal polarization. The implementation of the general conditions is being examined.

For the case of vertical polarization, clearly one condition on H_ϕ is given by equation (10*d*). The second condition may be obtained by manipulating Maxwell's equations and equation (10*b*) yielding

$$\frac{1}{\varepsilon_a}\frac{\partial}{\partial r}(r H_{\phi a}) = \frac{1}{\varepsilon_b}\frac{\partial}{\partial r}(r H_{\phi b}) \tag{11}$$

at the terrain surface. A third condition is also given by $\partial H_{\phi a}/\partial\theta = \partial H_{\phi b}/\partial\theta$ although this will not be used. For the case of horizontal polarization, equation (10*a*) will be one condition, and the second is obtained by manipulating Maxwell's equations and equation (10*e*) giving

$$\frac{\partial}{\partial r}(r E_{\phi a}) = \frac{\partial}{\partial r}(r E_{\phi b}) \tag{12}$$

at the terrain surface. The reason that the horizontal polarization case 'does not see' a discontinuity is because there is, in fact, no discontinuity in permeability at the surface.

We next use the flattening transformation defined in equations (4), and equations (11) and (12) to give

$$\frac{1}{\varepsilon_a}\left(\frac{H_{\phi a}}{r_e} + \frac{\partial H_{\phi a}}{\partial z}\right) = \frac{1}{\varepsilon_b}\left(\frac{H_{\phi b}}{r_e} + \frac{\partial H_{\phi b}}{\partial z}\right) \tag{13a}$$

and

$$\left(\frac{E_{\phi a}}{r_e} + \frac{\partial E_{\phi a}}{\partial z}\right) = \left(\frac{E_{\phi b}}{r_e} + \frac{\partial E_{\phi b}}{\partial z}\right). \tag{13b}$$

We now switch independent variables using equation (2). In the case of vertical polarization one derives from equation (10*d*)

$$n_a u_{Va} = n_b u_{Vb} \tag{14a}$$

while equation (13*a*) gives

$$\left(\frac{1}{n_a^2}\frac{\partial n_a}{\partial z}+\frac{1}{2n_a r_e}\right)u_{Va}+\frac{1}{n_a}\frac{\partial u_{Va}}{\partial z}=\left(\frac{1}{n_b^2}\frac{\partial n_b}{\partial z}+\frac{1}{2n_b r_e}\right)u_{Vb}+\frac{1}{n_b}\frac{\partial u_{Vb}}{\partial z}. \tag{14b}$$

Switching to modified refraction m, in using equation (7*b*) these equations become

$$m_a u_{Va}=m_b u_{Vb} \tag{15a}$$

and

$$\left(\frac{1}{m_b^2}\frac{\partial m_b}{\partial z}-\frac{1}{2m_b r_e}\right)u_{Vb}+\frac{1}{m_b}\frac{\partial u_{Vb}}{\partial z}=\left(\frac{1}{m_a^2}\frac{\partial m_a}{\partial z}-\frac{1}{2m_a r_e}\right)u_{Va}+\frac{1}{m_a}\frac{\partial u_{Va}}{\partial z}. \tag{15b}$$

For the case of horizontal polarization, use of equation (2*b*) and equations (10*a*) and (12) gives

$$u_{Ha}=u_{Hb} \qquad \text{and} \qquad \frac{\partial u_{Ha}}{\partial z}=\frac{\partial u_{Hb}}{\partial z}. \tag{16a, b}$$

For efficient numerical computation, the approach taken here treats the variable terrain in terms of staircase approximations using smooth earth formulae for the horizontal boundary conditions. The smooth earth boundary conditions are simplifications of the general boundary conditions for variable terrain. These conditions can be determined without approximations to the terrain, for the cases of vertical and horizontal polarization, in terms of directions normal and parallel to the terrain. Using a generalization of the earth flattening transformation that is applicable to the variable terrain, the general conditions can also be given in earth flattened coordinates (x, z). For brevity these formulae are not included.

We now discuss the discontinuity at vertical interfaces, whether real (due to range dependent changes in refraction) or numerical (due to stair case approximations to terrain slopes.) Any parabolic equation requires two conditions in height and one condition in range to determine a unique solution. We have just derived the two height conditions at horizontal interfaces for each polarization case. When considering the condition at vertical interfaces, once an initial field has been specified, at each step in range the typical condition is continuity of field. That is to say that when a set of loss values has been computed at a particular range step, these values are used as initial data for taking the next range step. This condition can be replaced by other possible more desirable conditions. We use results from scalar acoustic problems to derive a conservation of energy condition for the vertical interface [9–12].

The basic concept is to introduce a new dependent variable obtained by scaling the old variable. The scale could be height-dependent. In order to properly implement an energy-conserving condition at a vertical interface we must derive an expression for the energy flux in the range direction. We begin with the complex Poynting vector S, which is generally taken to give the flow of energy in a propagating electromagnetic field. The vector is defined as [1]

$$S=\tfrac{1}{2}E\times H^* \tag{17}$$

where the asterisk denotes complex conjugate. The average intensity of energy flow is taken as the real part of the complex Poynting vector. For the case of vertical polarization

$$S=\tfrac{1}{2}((E_\theta H_\phi^*)e_r-(E_r H_\phi^*)e_\theta). \tag{18}$$

The energy flux in the θ direction, denoted S_θ, is

$$S_\theta = -\tfrac{1}{2}\,\mathrm{Re}(E_r H_\phi^*). \tag{19}$$

Using Maxwell's equations and equation (2) in equation (19) gives

$$S_\theta = \frac{1}{2\omega\varepsilon_0 r^2 \sin\theta}\,\mathrm{Im}\left(\frac{\partial u_V}{\partial\theta}u_V^*\right). \tag{20}$$

In using equation (4) to switch to earth flattened coordinates the energy flux is given by

$$S_x = \frac{1}{2\omega\varepsilon_0 r_e}\exp\left(\frac{-2z}{r_e}\right)\mathrm{cosec}\left(\frac{x}{r_e}\right)\mathrm{Im}\left(\frac{\partial u_V}{\partial x}u_V^*\right). \tag{21}$$

The condition for conservation of energy along a vertical interface thereby becomes

$$\mathrm{Im}\left(\frac{\partial u_{V_{tr}}}{\partial x}u_{V_{tr}}^*\right) = \mathrm{Im}\left(\frac{\partial u_{V_{in}}}{\partial x}u_{V_{in}}^*\right) \tag{22}$$

where we use the subscript 'in' here to denote the incident wave while 'tr' denotes the transmitted wave.

This type of nonlinear boundary condition is quite difficult to implement in practice, however an equivalent linear condition can be derived. By factoring equation (8*a*), and retaining the outgoing solution, one can derive

$$\frac{\partial u_V}{\partial x} = \mathrm{i}k_0 Q_V u_V \tag{23a}$$

where

$$k_0 Q_V = \sqrt{\frac{\partial}{\partial z^2} + K_V^2}. \tag{23b}$$

Using equation (23) in equation (22) gives

$$\mathrm{Im}(\mathrm{i}Q_{V_{tr}}|u_{V_{tr}}|^2) = \mathrm{Im}(\mathrm{i}Q_{V_{in}}|u_{V_{in}}|^2) \tag{24a}$$

which will be satisfied if

$$Q_{V_{tr}}^{1/2}u_{V_{tr}} = Q_{V_{in}}^{1/2}u_{V_{in}}. \tag{24b}$$

One could in theory apply equation (24*b*) as the propagator for steps across vertical discontinuities. The simpler method of incorporating conservation conditions via a new dependent variable is derived by assuming negligible propagation angles. With this assumption, and those to follow, equations (8*b*) and (23*b*) yield the approximation $Q^{1/2} \approx (K_V^2/k_0^2)^{1/4} \approx \sqrt{m}$ so that the condition becomes

$$\sqrt{m_{tr}}u_{V_{tr}} = \sqrt{m_{in}}u_{V_{in}} \tag{25}$$

where m is a modified index of refraction defined by equation (9). In deriving equation (25), one must assume that the terms involving z derivatives of m^{-1} are negligible. We obtain here merely a first-order correction for conserving energy. If one desired, one could implement

the full correction, given in equation (24*b*) at each range step where there is a vertical discontinuity of some type. This compounds the numerical process, however, and slows down the algorithm significantly. It has been demonstrated that the first-order correction is sufficient for many types of environments when considering acoustic propagation [9]. Tests underway also tend to support this conclusion for electromagnetic problems as well.

Equation (25) suggests the transformation of dependent variable to be

$$w_V = \sqrt{m}u_V \tag{26}$$

and continuity of field in w will imply a first-order correction for conservation of energy in u. The case of horizontal polarization is analysed in a similar fashion leading to analogous results and a transformation identical to equation (25). For brevity, these results are omitted.

In using this transformation for conserving energy the elliptic equation that is solved is given as

$$\frac{\partial^2 w_i}{\partial x^2} + \sqrt{m}\frac{\partial^2}{\partial z^2}\left(\frac{w_i}{\sqrt{m}}\right) + K_i^2 w_i = 0 \tag{27}$$

where this equation has been derived by substituting equation (26) into equation (8*a*). In implementing the energy-conserving transformation one must now transform the interface conditions given in equations (15) and (16). For the case of vertical polarization conditions on w_V become

$$\sqrt{m_a}w_{Va} = \sqrt{m_b}w_{Vb} \tag{28a}$$

and

$$\frac{1}{2}\left(\frac{1}{m_a^{5/2}}\frac{\partial m_a}{\partial z} - \frac{1}{r_e m_a^{3/2}}\right)w_{Va} + \frac{1}{m_a^{3/2}}\frac{\partial w_{Va}}{\partial z} = \frac{1}{2}\left(\frac{1}{m_b^{5/2}}\frac{\partial m_b}{\partial z} - \frac{1}{r_e m_b^{3/2}}\right)w_{Vb} + \frac{1}{m_b^{3/2}}\frac{\partial w_{Vb}}{\partial z}. \tag{28b}$$

The conditions on w_H for the case of horizontal polarization become

$$\frac{1}{\sqrt{m_a}}w_{Ha} = \frac{1}{\sqrt{m_b}}w_{Hb} \tag{29a}$$

and

$$-\frac{1}{2m_a^{3/2}}\frac{\partial m_a}{\partial z}w_{Ha} + \frac{1}{\sqrt{m_a}}\frac{\partial w_{Ha}}{\partial z} = -\frac{1}{2m_b^{3/2}}\frac{\partial m_b}{\partial z}w_{Hb} + \frac{1}{\sqrt{m_b}}\frac{\partial w_{Hb}}{\partial z}. \tag{29b}$$

The preceding derivation has assumed that the complex part of m is small compared to the real part. This is true over most of the frequency regime and terrain cover of interest.

4. Numerical implementation

Our goal is to solve the differential equation, equation (27),

$$\frac{\partial^2 w_i}{\partial x^2} + \sqrt{m}\frac{\partial^2}{\partial z^2}\left(\frac{w_i}{\sqrt{m}}\right) + K_i^2 w_i = 0$$

subject to homogeneous Dirichlet conditions at the boundaries, and the interface conditions in equation (28) for vertical polarization or equation (29) for horizontal polarization. The modified wavenumber, K_i, is defined in equation (8*b*). For convenience in upcoming notation, we drop the i subscript in favour of the reader understanding that all results apply to both the vertical and horizontal polarization cases. This equation may be formally factored to give

$$\frac{\partial w}{\partial x} = ik_0\sqrt{1+Q}\,w \tag{30a}$$

where

$$k_0^2 Q = \sqrt{m}\frac{\partial^2}{\partial z^2}\frac{1}{\sqrt{m}} + K^2 - k_0^2 \tag{30b}$$

as the differential equation governing the outwardly propagating wave. The differences between this formulation and that in equation (23) is numerically motivated and will be discussed shortly. Removing the $\exp(ik_0x)$ from the solution u, equation (30*a*) becomes

$$\frac{\partial w}{\partial x} = ik_0\left(-1+\sqrt{1+Q}\right)w. \tag{31}$$

One may formally integrate equation (31) to give

$$w(x+\Delta x, z) = \exp\left(ik_0\Delta x\left(-1+\sqrt{1+Q}\right)\right)w(x,z). \tag{32}$$

Following the method of Collins we apply a Padé approximation [7]:

$$\exp\left(ik_0\Delta x\left(-1+\sqrt{1+Q}\right)\right) \cong 1+\sum_{l=1}^{np}\frac{a_{l,np}Q}{1+b_{l,np}Q} \tag{33}$$

where the coefficients $a_{l,np}$ and $b_{l,np}$ are determined numerically using the approach in [11]. The method used in [11] converges faster using the formulation in equation (30) than that in equation (23). The number np is the Padé number, or the number of terms used in the series approximation.

Substituting equation (33) into equation (32) one obtains the split-step Padé solution,

$$w(x+\Delta x, z) = w(x,z) + \sum_{l=1}^{np}\frac{a_{l,np}Qw(x,z)}{1+b_{l,np}Q}. \tag{34}$$

The terms in the sum may be computed in parallel, which is what makes this technique so appealing. That is we compute

$$\psi_l(x,z) = \frac{a_{l,np}Qw(x,z)}{1+b_{l,np}Q} \tag{35a}$$

in parallel and then calculate

$$w(x+\Delta x, z) = w(x,z) + \sum_{l=1}^{np}\psi_l(x,z). \tag{35b}$$

Let us discretize the problem as follows. First we will use a simple linear transformation to invert the problem so that z is measured positive down from the top of the atmosphere. For ease of notation we will still use the variable z rather than defining a new variable, say z'. Then we define a grid with mesh sizes $\mathrm{d}x$, and $\mathrm{d}z$. Let

$$w_j^n = w(n\,\mathrm{d}x,\ j\,\mathrm{d}z) \tag{36a}$$

and

$$\psi_{l,j}^n = \psi_l(n\,\mathrm{d}x,\ j\,\mathrm{d}z) \tag{36b}$$

When discretizing the differential operator Q, equation (35a) becomes a tridiagonal linear system of which the jth equation is

$$R1_{l,j}\psi_{l,j-1}^n + R2_{l,j}\psi_{l,j}^n + R3_{l,j}\psi_{l,j+1}^n = S1_{l,j}w_{j-1}^n + S2_{l,j}w_j^n + S3_{l,j}w_{j+1}^n \tag{37}$$

where $R1$, $R2$, $R3$, $S1$, $S2$, and $S3$, are dependent upon $\mathrm{d}z$ and medium properties through the function K and m. Once this system is solved for $\psi_{l,j}^n$ one uses equation (35b) to compute the solution w_j^{n+1} as

$$w_j^{n+1} = w_j^n + \sum_{l=1}^{np} \psi_{l,j}^n. \tag{38}$$

The numerical domain is terminated with homogeneous Dirichlet conditions on the field w. To avoid spurious reflections from the top of the atmosphere, an absorbing layer is introduced with complex wavenumber. Similarly, at the bottom of the earth layer, one increases conductivity so as to eliminate reflections. For most typical ground cover with non-zero conductivity the Earth acts as an absorbing layer naturally. Increasing conductivity near the bottom of the domain insures no reflections. As for implementing the interface conditions as given in equations (28) and (29) one uses the idea of virtual points [11]. Assume the atmosphere–terrain interface occurs between the jth and $(j+1)$th notch points. We place two virtual points a′ and b′ in between the two actual points, such that the point a′(b′) represents the continuation of the atmospheric (terrain) solution one notch point.

This technique is described fully in [10]. By requiring each $\psi_{l,j}^n$ to satisfy the linear interface conditions at the earth's surface, one automatically satisfies the interface requirement on the entire solution w_j^n. The discretized equations at the nodes on each side of the interface are

$$R1_{l,j}\psi_{l,j-1}^n + R2_{l,j}\psi_{l,j}^n + R3_{l,j}\psi_{l,\mathrm{a}'}^n = S1_{l,j}w_{j-1}^n + S2_{l,j}w_j^n + S3_{l,j}w_{\mathrm{a}'}^n \tag{39a}$$

and

$$R1_{l,j+1}\psi_{l,\mathrm{b}'}^n + R2_{l,j+1}\psi_{l,j+1}^n + R3_{l,j+1}\psi_{l,j+2}^n = S1_{l,j+1}w_{\mathrm{b}'}^n + S2_{l,j+1}w_{j+1}^n + S3_{l,j+1}w_{j+2}^n \tag{39b}$$

We approximate

$$w_{\mathrm{a}} = \tfrac{1}{2}(w_j^n + w_{\mathrm{a}'}^n) \qquad w_{\mathrm{b}} = \tfrac{1}{2}(w_{j+1}^n + w_{\mathrm{b}'}^n) \tag{40a, b}$$

$$\frac{\partial w_{\mathrm{a}}}{\partial z} = \frac{w_{\mathrm{a}'}^n - w_j^n}{\mathrm{d}z} \quad \text{and} \quad \frac{\partial w_{\mathrm{b}}}{\partial z} = \frac{w_{j+1}^n - w_{\mathrm{b}'}^n}{\mathrm{d}z} \tag{40c, d}$$

at the interface, and substituting these expressions in equation (28) for vertical polarization or equation (29) for horizontal polarization allows one to solve for the virtual point solutions in terms of actual notch point solutions. For the case of vertical polarization, using equation (40) in equation (28) gives

$$A_1(w_j^n + w_{a'}^n) = A_2(w_{j+1}^n + w_{b'}^n) \tag{41a}$$

and

$$A_3(w_j^n + w_{a'}^n) + A_4(w_{a'}^n - w_j^n) = A_5(w_{j+1}^n + w_{b'}^n) + A_6(w_{j+1}^n - w_{b'}^n) \tag{41b}$$

where

$$A_1 = \sqrt{m_a} \qquad A_2 = \sqrt{m_b} \tag{41c,d}$$

$$A_3 = \frac{dz}{4}\left(\frac{1}{r_e m_a^{3/2}} + \frac{1}{m_a^{5/2}}\frac{\partial m_a}{\partial z}\right) \qquad A_4 = \frac{1}{m_a^{3/2}} \tag{41e,f}$$

$$A_5 = \frac{dz}{4}\left(\frac{1}{r_e m_b^{3/2}} + \frac{1}{m_b^{5/2}}\frac{\partial m_b}{\partial z}\right) \qquad \text{and} \qquad A_6 = \frac{1}{m_b^{3/2}}. \tag{41g,h}$$

Solving equations (41*a*) and (41*b*) for the virtual solutions gives

$$w_{a'}^n = \alpha_{11} w_j^n + \alpha_{12} w_{j+1}^n \tag{42a}$$

and

$$w_{b'}^n = \alpha_{21} w_j^n + \alpha_{22} w_{j+1}^n \tag{42b}$$

where

$$\alpha_{11} = (A_1(A_5 - A_6) + A_2(A_4 - A_3))/(A_1(A_6 - A_5) + A_2(A_3 + A_4)) \tag{42c}$$

$$\alpha_{12} = (2A_2A_6)/(A_1(A_6 - A_5) + A_2(A_3 + A_4)) \tag{42d}$$

$$\alpha_{21} = (2A_1A_4)/(A_1(A_6 - A_5) + A_2(A_3 + A_4)) \tag{42e}$$

and

$$\alpha_{22} = (A_1(A_5 + A_6) - A_2(A_3 + A_4))/(A_1(A_6 - A_5) + A_2(A_3 + A_4)). \tag{42f}$$

One may also repeat this procedure for each individual $\psi_{l,j}^n$, and since they each satisfy the same interface conditions one uses equation (42) exactly for virtual point solutions $\psi_{l,a'}^n$ and $\psi_{l,b'}^n$. The result is that at the interface equation (39) becomes

$$\begin{aligned} R1_{l,j}\psi_{l,j-1}^n + (R2_{l,j} + \alpha_{11}R3_{l,j})\psi_{l,j}^n + \alpha_{12}R3_{l,j}\psi_{l,j+1}^n \\ = S1_{l,j}w_{j-1}^n + (S2_{l,j} + \alpha_{11}S3_{l,j})w_j^n + \alpha_{12}S3_{l,j}w_{j+1}^n, \end{aligned} \tag{43a}$$

and

$$\begin{aligned} \alpha_{21}R1_{l,j+1}\psi_{l,j}^n + (R2_{l,j+1} + \alpha_{22}R1_{l,j+1})\psi_{l,j+1}^n + R3_{l,j+1}\psi_{l,j+2}^n \\ = \alpha_{21}S1_{l,j+1}w_j^n + (S2_{l,j+1} + \alpha_{22}S1_{l,j+1})w_{j+1}^n + S3_{l,j+1}w_{j+2}^n. \end{aligned} \tag{43b}$$

A similar analysis in the horizontal polarization case yields very similar results in terms of equation (43), with differences in the definitions of the α_{ij} coefficients. Using equation (40) in equation (29) gives the equations

$$\bar{A}_1(w_j^n + w_{a'}^n) = \bar{A}_2(w_{j+1}^n + w_{b'}^n) \tag{44a}$$

and

$$\bar{A}_3(w_j^n + w_{a'}^n) + \bar{A}_1(w_{a'}^n - w_j^n) = \bar{A}_4(w_{j+1}^n + w_{b'}^n) + \bar{A}_2(w_{j+1}^n - w_{b'}^n) \tag{44b}$$

where now

$$\bar{A}_1 = \frac{1}{\sqrt{m_a}} \qquad \bar{A}_2 = \frac{1}{\sqrt{m_b}} \tag{44c, d}$$

$$\bar{A}_3 = -\frac{1}{4m_a^{3/2}}\frac{\partial m_a}{\partial z} \quad \text{and} \quad \bar{A}_4 = -\frac{1}{4m_b^{3/2}}\frac{\partial m_b}{\partial z}. \tag{44e,f}$$

Solving equations (44*a*) and (44*b*) for $w_{a'}^n$ and $w_{b'}^n$ yields

$$w_{a'}^n = \bar{\alpha}_{11} w_j^n + \bar{\alpha}_{12} w_{j+1}^n \tag{45a}$$

and

$$w_{b'}^n = \bar{\alpha}_{21} w_j^n + \bar{\alpha}_{22} w_{j+1}^n \tag{45b}$$

where

$$\bar{\alpha}_{11} = \bar{\alpha}_{22} = (\bar{A}_1\bar{A}_4 - \bar{A}_2\bar{A}_3)/(2\bar{A}_1\bar{A}_2 + \bar{A}_2\bar{A}_3 - \bar{A}_1\bar{A}_4) \tag{45c}$$

$$\bar{\alpha}_{12} = (2\bar{A}_2^2)/(2\bar{A}_1\bar{A}_2 + \bar{A}_2\bar{A}_3 - \bar{A}_1\bar{A}_4) \tag{45d}$$

and

$$\bar{\alpha}_{21} = (2\bar{A}_1^2)/(2\bar{A}_1\bar{A}_2 + \bar{A}_2\bar{A}_3 - \bar{A}_1\bar{A}_4). \tag{45e}$$

The final implementation is exactly that in equation (43) with α_{ij} being replaced by $\bar{\alpha}_{ij}$.

Therefore the numerical implementation of the terrain interface is a simple modification of the algorithm at the jth and $(j+1)$th nodes. The code SSP is currently undergoing testing. The next section discusses preliminary testing and evaluation of SSP including the atmosphere–terrain interface implementation.

5. Numerical examples

The numerical code SSP is currently being tested. The results presented in this paper do not utilize the advantage of parallel processing. Preliminary solutions were calculated on PCs simply to test the code and demonstrate certain aspects of this method. The final program will be run on a parallel machine. References [8–10] suggest run time speeds 100 times faster than conventional methods.

Since the implementation of interface matching conditions is an integral part of the program, examination of the numerical methods used there is critical. While some acoustic propagation models do incorporate horizontal interfaces many more do not. It seems that the discontinuity in the acoustic case is slight as compared to the EM case. So slight as to permit one to smooth out discontinuities or simply ignore them altogether. This is certainly not the case for electromagnetic propagation. A series of tests, too comprehensive to present here, have examined this aspect of the problem. By altering acoustic parameters so as to have a discontinuity of order similar to the EM case, the results show that one must also incorporate the acoustic matching conditions to have accurate solutions.

The simplest analytical model to test the method is the Lloyds mirror problem, in which the medium is taken as homogeneous, with homogeneous Dirichlet conditions at the top and bottom of the domain. The source frequency is taken as 4.99 MHz, with $dr = 2$ m, and $dz = 0.5$ m. The source and receiver height are both taken to be 75 m, and the entire thickness of the domain is 200 m. Figure 1(a) shows a comparison of the propagation losses as computed by the program SSP (full curve) and the program EFEPE (dotted). The code EFEPE is the original acoustic code and was benchmarked against a normal mode program showing excellent agreement [7]. As one can see there is virtually no difference in solutions. We were satisfied that the EM adaptation was coded correctly. We next considered the interface modelling. We are currently looking into benchmark models for EM propagation so as to fully test the numerical implementation of the interface matching conditions. However, there are existing acoustic benchmark models available immediately. We are able to implement acoustic boundary conditions, similar to our electromagnetic conditions, in the code and compare them to results that were benchmarked against normal mode solutions. The model we choose is called Case 3b from the NORDA Parabolic Equation Workshop [13]. It is basically one homogeneous medium overlying a different homogeneous medium with absorption. The density discontinuity at the ocean–sea floor interface is very similar to the light speed discontinuity in the EM problem at the atmosphere–terrain interface. While the interface conditions for the acoustic model are not as complicated as the EM problem, the numerical implementation using virtual points is identical.

Having implemented the interface conditions in the acoustic code, figure 1(b) compares the results from SSP (full) and the original acoustic program EFEPE (dotted,) which was benchmarked against a normal mode solution. The output from EFEPE was in excellent agreement with the normal mode solution except at null locations, specifically the one near 7 km. While there are subtle differences in losses, they are at most 1 dB, and the curves generally agree quite well. Work is currently underway to test the EM interface conditions.

The remaining figures demonstrate the method's ability to greatly increase range step size. We will use the Lloyds mirror example to illustrate. Using the EFEPE result in figure 1(a) as a benchmark we have calculated the solution using the code SSP with $np = 4$ and $dr = 50$ m. Figure 2(a) shows the results with fair agreement that decays as range increases. When increasing np to 8, as in figure 2(b), excellent accuracy is obtained. For parallel computations this could mean very little extra run time achieving much better accuracy. When the range step is increased to 100 m, as in figure 3(a), the accuracy is still maintained for $np = 8$. When the range step is increased to 200 m, the accuracy begins to degrade. Finally, when increasing np to 10, shown in figure 4, accuracy, while still not perfect, is increased greatly.

In theory, one can take very large range steps when using this method. One need only take np large enough so that the Padé approximation gets arbitrarily accurate. However, the limiting factor will be terrain and atmospheric conditions. Taking range steps too large could result in 'stepping over mountains'. As is typical with parabolic approximation methods,

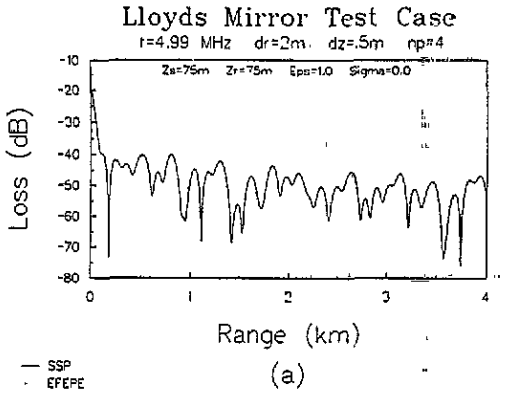

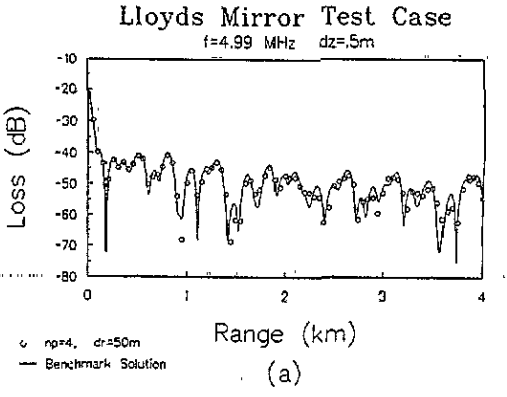

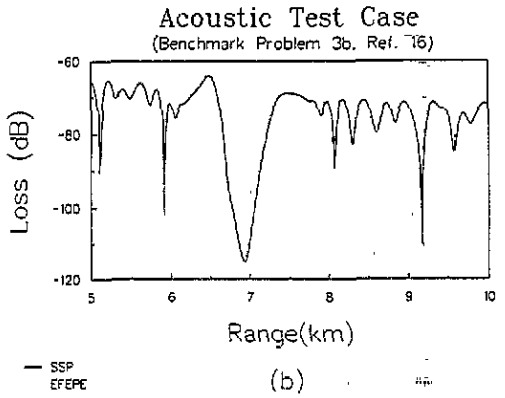

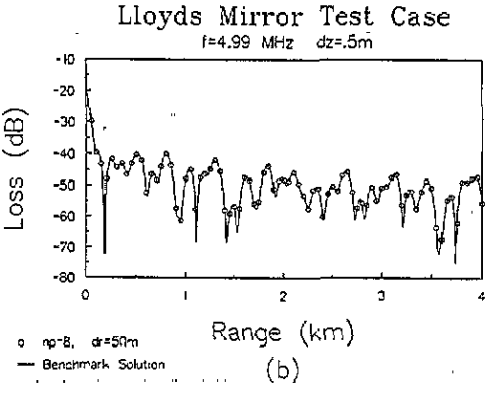

Figure 1. (a) The Lloyds mirror test problem. Source and receiver height are 75 m, and source frequency is 4.99 MHz. Intensity loss in dB is plotted against range in km. SSP (full curve) and EFEPE (dotted curve) show excellent agreement. (b) Acoustic benchmark Case 3b in [13]: SSP (full curve) and EFEPE (dotted curve) show excellent agreement.

Figure 2. Lloyds mirror test problem: comparison of SSP with benchmark solution for (a) $np = 4$ and $dr = 50$ m, and (b) $np = 8$, and $dr = 50$ m.

the range-dependent problem is sectored into range-independent slabs. Discretization of a continuous medium results in staircase effects. These effects are minimized by taking smaller range steps. Therefore there is still a lot of work to be done in the delicate matter of trading off time (dr and np as large as possible) and accuracy (dr small enough to capture the true physical properties of the medium). Sensitivity testing and benchmarking are crucial aspects of this problem and current efforts are being placed on these areas.

6. Summary

Scalar Helmholtz equations have been derived directly from Maxwell's equations for the cases of vertical and horizontal polarization. The primary assumption necessary for such a reduction is that the medium is approximately symmetric in one spatial direction. Factorization of these equations yield parabolic equations which are then symbolically

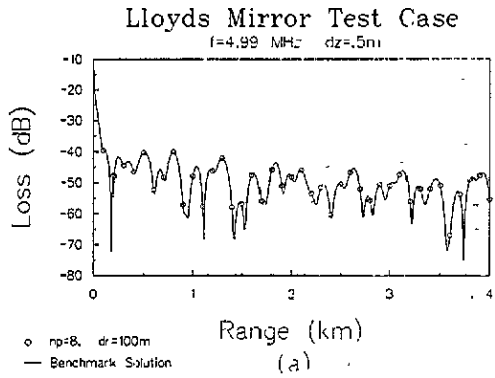

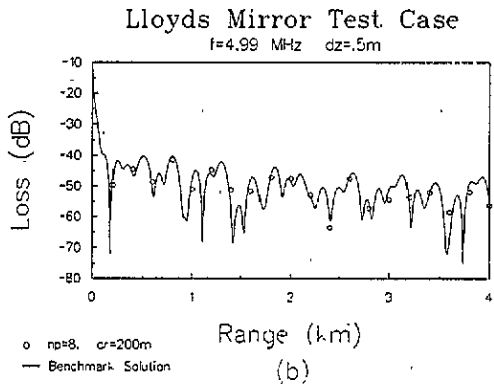

Figure 3. Lloyds mirror test problem: comparison of SSP with benchmark solution for (a) $np = 8$ and $dr = 100$ m, and (b) $np = 8$, and $dr = 200$ m.

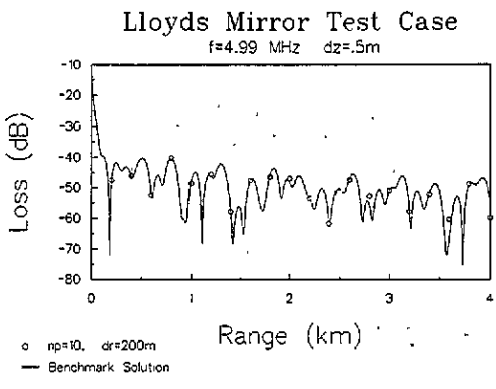

Figure 4. Lloyds mirror test problem: comparison of SSP with benchmark solution for $np = 10$ and $dr = 200$ m.

solved in the range direction. What one obtains is a symbolic expression for the range-stepping macroscopic operator. Rather than discretize the microscopic operator, a Padé series approximation is used for the macroscopic operator. In theory this allows very large range steps. Step size is still ultimately determined by medium characteristics. However there are numerical advantages over typical finite difference methods, the main being the suitability of the method to be parallelized for multi-processor computers.

Interface conditions have been fully developed for linking the atmosphere to the ground. Methods for conserving energy at vertical interfaces has also been discussed, with the result that to first order, a simple transformation of dependent variable allows for implementation. This will provide corrections to sloping terrain errors as well as range-dependent refractive effects. The numerical implementation of the split-step Padé solution and interface conditions has also been presented. Several benchmark calculations and interface modelling comparisons were also presented. A full description of the code SSP is contained in technical reports available from the authors upon request. The user's manual includes program flow charts, input descriptions and output options. Also described in this report is a post processing graphics program called GRAPH. This program produces contour graphs for visual display only.

Acknowledgments

This work has been funded by the Joint Electronic Warfare Center (now the Joint Command and Control Warfare Center), Kelly AFB San Antonio, TX. The authors wish to thank Dr Michael Collins for many hours of help in our adapting his original acoustic code to the electromagnetic problem. The authors also wish to acknowledge the work of Frank Ryan in his technical note 'Analysis of electromagnetic propagation over variable terrain using the parabolic wave equation' *NOSC Technical Report* 1453, 1991.

References

[1] Stratton J A 1941 *Electromagnetic Theory* (New York: McGraw-Hill)

[2] Tappert F D 1977 The parabolic approximation method *Wave Propagation and Underwater Acoustics (Lecture Notes in Physics 70)* ed Joseph B Keller and John S Papadakis (New York: Springer) pp 224–87

[3] Lee D, Botseas G and Papdakis J 1981 Finite difference solutions to the parabolic wave equations *J. Acoust. Soc. Am.* **70** 795–800

[4] Hardin R H and Tappert F D 1973 Application of the split-step Fourier method to the numerical solution of nonlinear and variable coefficient wave equations *SIAM Rev.* **15** 423

[5] Ko H W, Sari J W and Skura J P 1983 Anomalous microwave propagation through atmospheric ducts *Johns Hopkins APL Tech. Dig.* **4** 12–26

[6] Lee D and Saied F 1990 A fourth-order difference scheme to improve the computational speed of wide angle propagation *Computational Acoustics* vol 1, ed D Lee, A Cakmak and R Vichnevetsky (New York: North-Holland) pp 27–35

[7] Collins M D 1993 A split-step Padé solution for the parabolic equation method *J. Acoust. Soc. Am.* **93** 1736–42

[8] Collins M D 1993 The adiabatic mode parabolic equation *J. Acoust. Soc. Am.* **94** 2269–78

[9] Collins M D 1991 A higher-order energy conserving parabolic equation for range-dependent ocean depth, sound speed, and density *J. Acoust. Soc. Am.* **89** 1068–75

[10] Collins M D 1993 An energy-conserving parabolic equation for elastic media *J. Acoust. Soc. Am.* **94** 975–82

[11] Collins M D 1989 A higher-order parabolic equation for wave propagation in an ocean overlying an elastic bottom *J. Acoust. Soc. Am.* **86** 1459–64

[12] Collins M D 1992 A two-way parabolic equations for acoustic backscatter in the ocean *J. Acoust. Soc. Am.* **91** 1357–68

[13] Davis J A, White D and Cavanagh R C 1982 NORDA Parabolic Equation Workshop *NORDA Technical Note (September)* 143